

A SLOPE-BASIN MODEL FOR EARLY PALEOGENE DEEP-WATER SEDIMENTATION (ACHTHAL FORMATION NOV. NOM.) AT THE TETHYAN CONTINENTAL MARGIN (ULTRAHELVETIC REALM) OF THE EUROPEAN PLATE (EASTERN ALPS, GERMANY)

Hans EGGER^{1*)} & Omar MOHAMED²⁾³⁾

KEYWORDS

Northwestern Tethys
Upper Cretaceous
Lower Paleogene
Ultrahelvetic unit
nannoplankton
dinoflagellates
Eastern Alps
slope-basin

¹⁾ Geological Survey of Austria, Neulinggasse 38, 1030 Vienna, Austria;

²⁾ University of Graz, Institut of Earth Sciences, Heinrichstraße 26, 8010 Graz, Austria;

³⁾ Geology Department, Faculty of Science, El-Minia University, El-Minia, Egypt;

^{*} Corresponding author, hans.egger@geologie.ac.at

ABSTRACT

A ca. 320 m thick composite section (Goppling section) of a turbidite-rich deep-water system outcropping between Teisendorf and Oberteisendorf (Bavaria) encompasses the upper Maastrichtian to Ypresian (calcareous nannoplankton Zones CC25 to NP11). These deposits conformably overlie red clayey marlstone (Buntmergelserie). The whole succession is part of the Ultrahelvetic thrust unit, which is a detached part of the continental margin of the southern European Plate. In the latest Maastrichtian and early Paleogene, subsidence to below the calcite compensation depth coeval with the onset of turbidite sedimentation indicates the development of slope-basins by subsiding crustal fault blocks. These basins acted as sediment traps and caused a dearth of turbidite sedimentation in the adjoining Penninic basin. During the Danian, turbidites in the Goppling slope-basin were deposited from currents, that flowed parallel with the E-W-trending basin axis and the strike of the slope. In the Selandian, sedimentation rates outpaced subsidence rates and the basin filled up to the spill-point. This is indicated by a shift in the section from sand-rich to mud-rich lithologies and a change from basin-axial to downslope (N-S) paleotransport directions. Turbidites were deposited on the smooth bathymetry of the filled basin due to the reduction of slope gradient. Another pulse of subsidence formed a new depression at this site in the Ypresian and caused the deposition of a sand-rich turbidite succession from longitudinal flowing turbidity currents. For the entire deep-water system overlying the Buntmergelserie, the new lithostratigraphic term Achthal Formation is introduced.

Aus dem Gebiet von Teisendorf und Oberteisendorf (Oberbayern) wird ein ca. 320 m mächtiges Tiefwasserablagerungssystem beschrieben, das einen stratigraphischen Umfang vom obersten Maastrichtium bis ins Ypresium (kalkige Nannoplankton-Zonen CC25 bis NP11) aufweist. Diese Ablagerungen liegen mit einem ungestörten stratigraphischen Kontakt auf roten mergeligen Tonsteinen der Buntmergelserie. Die gesamte Abfolge (Goppling-Profil) wird dem Ultrahelvetikum zugerechnet und als abgescherter Teil des Kontinentalrandes der südlichen Europäischen Platte interpretiert. Im späten Maastrichtium und frühen Paläogen deuten die Absenkung des Bodens des Sedimentationsraumes unter die Kalzitkompensationstiefe und die zeitgleich einsetzende Turbiditsedimentation auf die Absenkung von Krustenschollen hin, die zur Entstehung von Hangbecken führten. Diese Becken waren Sedimentfallen und bewirkten einen weitgehenden Ausfall der Turbiditsedimentation im benachbarten Penninischen Becken. Die Turbidite im Danium des Goppling-Profiles wurden aus becken- und hangparallelen Trübeströmen abgesetzt. Im Selandium überstiegen die Sedimentationsraten die Subsidenzraten und das Becken wurde bis an den Rand der begrenzenden Schwelle aufgefüllt. Die hangparallel transportierten Sandsteine der Beckenfüllung werden von einer pelitreichen Abfolge überlagert, deren Turbidite senkrecht zum Hangstreichen transportiert wurden. Das aufgefüllte Becken bildete eine Verebnung am Hang, wo es aufgrund des Gefälleverlustes zur Turbiditsedimentation kam. Eine neuerliche Absenkung führte im Ypresium wieder zur Bildung eines kleinen Beckens, das von sandreichen Turbiditen aus beckenparallel fließenden Trübeströmen aufgefüllt wurde. Für die gesamte im stratigraphisch Hangenden der Buntmergelserie vorkommende Tiefwasserabfolge wird die neue lithostratigraphische Bezeichnung Achthal-Formation vorgeschlagen.

1. INTRODUCTION

The northern rim of the fold-and-thrust belt of the Eastern Alps consists of detached Cretaceous to Paleogene deposits, that tectonically overlie the sedimentary infill of the Alpine Molasse Basin. From north to south, these thrust units originate from (1) the southern shelf of the European Plate (Helvetic unit), (2) the adjacent south-facing passive continental margin (Ultrahelvetic unit) and (3) the abyssal Penninic Basin (Rhenodanubian Flysch Zone). Thrusting and wrenching from the late

Eocene onwards disturbed the original configuration of the passive margin deposits and complicated the relationship to their source areas.

Depending on the paleodepth of the slope, the pelitic rocks of the Ultrahelvetic unit display varying carbonate contents. Prey (1952, 1953) combined these pelitic deposits into Buntmergelserie, an informal lithostratigraphic unit that was thought to comprise the Albian to upper Eocene. Remarkably, only a

very few and small outcrops of Paleocene to lower Eocene deposits have been recognized, most of which have unclear tectonic positions due to a strong tectonic overprint. Reworking of older Paleogene rocks in the Eocene has been proposed as a possible reason for the rare occurrence of lower Paleogene deposits in the Ultrahelvetetic thrust unit (Widder, 1988).

Hagn (1960; 1967) was the first to designate a sandstone succession ("Achthaler Sandstein" of Gumbel, 1862) to the Paleocene of the lower bathyal to abyssal southern Ultrahelvetetic sedimentation area, based on agglutinating foraminifera. However, a more precise age for this lithostratigraphic unit, and its relationship to the bordering Buntmergelerde remains unclear (Freimoser, 1972).

In this paper, the first continuous upper Maastrichtian to Ypresian stratigraphic record in the Ultrahelvetetic unit is documented. Biostratigraphy based primarily on calcareous nannoplankton. To increase the stratigraphical resolution around the Cretaceous/Paleogene-boundary dinoflagellate cyst assemblages were examined. The aim of the paper is to evaluate the sedimentation area of these upper Cretaceous to lower Paleogene deposits, which consist essentially of siliciclastic turbidites, and elucidates the tectonic evolution of the European continental margin in the Paleogene.

2. MATERIAL AND METHODS

In the forest south of Teisendorf and Oberteisendorf, a number of small creeks have created excellent exposures of Ultrahelvetetic rocks. Almost all such outcrops lie to the south of the hiking trail running between the two villages. For better orientation, the more important creeks have been numbered (Fig. 1).

In total, 55 smear slides were studied with the light microscope at a magnification of 1000x for calcareous nannoplankton and classified with the Standard Tertiary zonation (NP-zonation) of Martini (1971) and the CC-zonal scheme for the Cretaceous of Sissingh (1977). The slides are housed in the collection of the Geological Survey of Austria. In general, the nannoplankton assemblages are poorly preserved, particularly strongly fragmented, and thus show low diversity. In the upper Maastrichtian all species show rare occurrences with the exception of *Micula staurophora*. This species is less prone to dissolution and occurs with 1-10 specimens per field of view (spfv) in the slides. *Arkhangelskiella cymbiformis* is the second-most frequent species with a single specimen in 1-10 fields of view. All other species occur with single specimens in 10-100 fields of view. The Paleogene assemblages show a similar preservation quality as the Maastrichtian ones.

The better preserved samples are dominated by *Coccolithus pelagicus* and *Toweius* spp. (mainly *T. callosus* and minor occurrences of *T. occultatus* and *T. pertusus*), which occur with 1-10 spfv. Sphenolithids are relatively common in the Eocene samples (1 specimen in 1-10 fv), whereas discoasterids are strongly corroded and rare throughout that part of the section.

To obtain a better stratigraphic resolution around the Cretaceous/Paleogene-boundary (K/Pg-boundary), nine samples were also studied for dinoflagellates. The readers are referred to Fensome et al. (2008) for taxonomy and references of taxa. The samples were processed at the Institute of Earth Science, Graz University following standard procedures for palynological preparations. Twenty grams of each sample were treated by hydrochloric acid (HCl 36%) to remove carbonate, and hydrofluoric acid (HF 40%) to remove siliclastic material. The re-

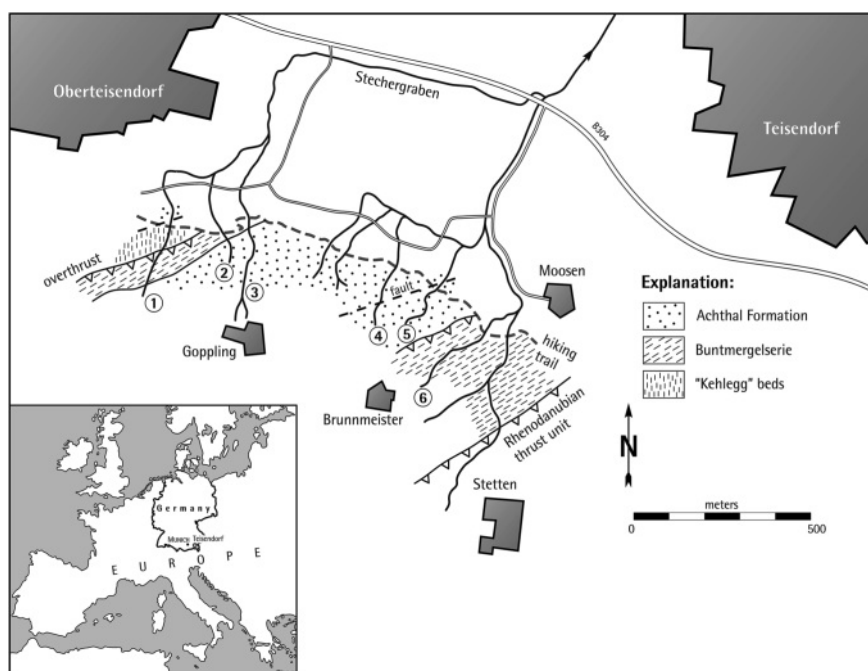


FIGURE 1: Sketch map of the area investigated. Numbers indicate the most important creek sections mentioned in the text.

sidue was sieved on 20 µm nylon sieves. The palynodebris was mounted in glycerine jelly on microscope slides and sealed for examination under a transmitted light microscope. All dinoflagellate slides are stored in the Institute of Earth Science, Graz University.

In general, the dinoflagellates show moderate preservation. Diversity is relatively high in the Upper Maastrichtian samples (TS) compared to the Danian samples (Ach) and ranges from 1 species per sample in Ach 3/09 to 27 species per sample in TS 11/09. The average diversity in the six TS samples is 20 species per sample and 11 species per sample in the three Ach samples. The stratigraphic distribution of dinoflagellate taxa in the Goppling section is shown in Table 1. Together with Kirsch (1991) and Kuhn & Kirsch (1992), these are the only dinoflagellate data from the Ultrahelvetetic domain.

3. GEOLOGICAL SETTING

The Ultrahelvetic thrust unit in the investigated area (Fig. 1) is composed of three tectonic slices exposing beds continuously dipping to the southeast. The ca. 320 m thick section described in here is the sedimentary succession of the Goppling slice, encompassing Maastrichtian to Lower Eocene deposits. Along the course of creek 1, the Goppling slice has been thrust over dark-grey silty marlstone and claystone with intervening turbiditic sandstone beds of the Oberteisendorf slice. These deposits, which are of Danian age (calcareous nannoplankton Zone NP3 – *Chiasmolithus danicus* Zone), resemble the Kehlegg beds in western Austria (Oberhauser, 1991). This lithostratigraphic unit originates from a part of the Ultrahelvetic slope (northern Ultrahelvetic area) less deep than the depositional area of the Goppling section (southern Ultrahelvetic area).

The strongly deformed Brunmeister slice is the tectonically highest slice of the Ultrahelvetic thrust unit and is overthrust by Lower Cretaceous deposits of the Penninic Rhenodanubian thrust unit. The Brunmeister slice rests tectonically on the Goppling slice and consists of brick-red colored marly deposits (Buntmergelserie) of predominantly Campanian age. Occasionally, debris flow deposits are intercalated in the marlstone. For example, in the upper part of creek 6, a ca. 1.5 m thick debris flow contains rounded clasts of light grey limestone and sub-rounded clasts of chlorite-schist with diameters up to 15 cm, floating in a grey marly matrix. The co-occurrence of *Reinhardtites levis*, *Uniplanarius trifidus*, *Broinsonia parca constricta* and *Eiffelithus eximius* in slump matrix (sample Stetten 2) indicates the lower Upper Campanian calcareous nannoplankton Subzone CC22b. The preservation of the nannoplankton assemblages of the surrounding autochthonous deposits is worse (samples Stetten 1 and 3). In the strongly corroded and fragmented nanoflora several specimens of *Ceratolithoides aculeus* were found, a species that has its lowest occurrence in the Campanian Zone CC20.

4. STRATIGRAPHIC RESULTS FROM THE GOPPLING SECTION

4.1 MAASTRICHTIAN

The basal part of the Goppling section is formed by ca. 50 m of bioturbated red clayey marlstone, which is assigned to the Buntmergelserie. The top of this red-bed succession is exposed in creek 3 ("Goppling creek"), immediately south of the hiking trail bridge (Fig. 2/1). There, the marlstone contains 19 wt% carbonate. The nannoplankton assemblages are dominated by *Micula staurophora*, whereas all other species are rare and most specimens are preserved only as fragments. Apart from *Lithraphidites quadratus*, the zonal marker for the upper Maastrichtian Zone CC25, *Arkhangelskiella cymbiformis* (Fig.

TABLE 1: Distribution of dinoflagellate taxa in the Goppling section. The arrangement of taxa is according to the first occurrence and alphabetical order. Key dinoflagellate species are shaded.

Maastrichtian						Paleogene			Age
TS 4/09	TS 8/09	TS 11/09	TS 12/09	TS 13/09	TS 14/09	Ach 1/09	Ach 2/09	Ach 3/09	Sample Number
*									1 <i>Cyclonephellium compactum</i>
*									2 <i>Membranilamacia</i> sp.
*									3 <i>Rigaudella aemula</i>
*	*								4 <i>Pterodinium aliferum</i>
*	*	*							5 <i>Glaphyrocysta perforata</i>
*	*	*	*						6 <i>Hystrichostrogylon membraniphorum</i>
*	*	*		*					7 <i>Cribroperidinium cooksoniae</i>
*	*	*		*					8 <i>Dinogymnium acuminatum</i>
*	*			*	*				9 <i>Heterosphaeridium cordiforme</i>
*	*	*	*	*	*				10 <i>Hystrichosphaeridium salpingophoru</i>
*	*			*	*				11 <i>Pyxidinospis</i> sp.
*	*	*	*	*	*				12 <i>Pterodinium cingulatum</i> subsp. <i>cingulatum</i>
*	*	*	*	*	*				13 <i>Spiniferites pseudofurcatus</i>
*	*	*	*	*	*	*			14 <i>Achomosphaera ramulifera</i>
*	*	*		*		*			15 <i>Spiniferites membranaceus</i>
*	*	*	*		*	*	*		16 <i>Cordosphaeridium fibrospinosum</i>
*		*				*	*		17 <i>Glaphyrocysta semitecta</i>
*	*	*			*		*		18 <i>Operculodinium centrocarpum</i>
*	*	*	*	*	*	*	*		19 <i>Palynodinium grillator</i>
*	*	*	*	*	*		*		20 <i>Spiniferites ramosus</i>
*		*	*			*			21 <i>Spiniferites ramosus</i> subsp. <i>granosus</i>
*						*	*		22 <i>Thalassiphora pelagica</i>
*	*	*	*	*		*	*		23 <i>Areoligera senonensis</i>
*									24 <i>Cordosphaeridium</i> sp.
*						R			25 <i>Disphaerogena carposphaeropsis</i>
*									26 <i>Exochosphaeridium bifidum</i>
*	*								27 <i>Dinogymnium</i> sp.
*	*								28 <i>Surculosphaeridium longifurcatum</i>
*	*								29 <i>Trithyrodinium suspectum</i>
*		*							30 <i>Trabeculidium quinquetrum</i>
*	*	*	*	*	*	*	*		31 <i>Areoligera coronata</i>
*						*	*		32 <i>Areoligera volata</i>
	*								33 <i>Achilleodinium biformoides</i>
		*							34 <i>Cerodinium diebelii</i>
		*							35 <i>Cerodinium</i> sp.
		*							36 <i>Palaeocystodinium lidiae</i>
	*	*							37 <i>Areoligera gippingensis</i>
	*					*			38 <i>Rigaudella apenninica</i>
	*						*		39 <i>Areoligera guembelii</i>
		*							40 <i>Aptodinium deflandrei</i>
		*		*					41 <i>Hystrichosphaeridium tubiferum</i>
		*				*	*		42 <i>Oligosphaeridium complex</i>
			*						43 <i>Achomosphaera</i> cf. <i>allicornu</i>
			*						44 <i>Adnatosphaeridium filiferum</i>
			*						45 <i>Coronifera oceanica</i> subsp. <i>hebospina</i>
			*						46 <i>Palynodinium minus</i>
			*	*					47 <i>Impagidinium?</i> <i>ovum</i>
			*		*				48 <i>Cordosphaeridium inodes</i>
					*				49 <i>Carpatella comuta</i>
					*				50 <i>Damassadinium californicum</i>
					*				51 <i>Palaeoperidinium pyrophorum</i>
					*				52 <i>Spongodinium delitiense</i>
					*	*			53 <i>Riculacysta amplexa</i>
						*			54 <i>Lejeunecysta</i> sp.
						*			55 <i>Senoniasphaera inornata</i>



FIGURE 2: Sedimentary facies at the Goppling section. 1) Buntmergelerde, Upper Maastrichtian (CC25), creek 3; 2) Sandstone beds of lower Danian age, creek 3; 3 and 4) Danian sandstone and intervening red claystone, creek 3; 5) The highest red claystone layers, upper Danian (NP3-4), creek 3; 6) Thick-bedded sandstone, Selandian (NP5); 7) Mud-rich facies with abundant bioturbated green hemipelagic claystone and thin turbiditic sandstone. Note the erosional channels perpendicular to the trend of the strike (Selandian-Thanetian), creek 3; 8) Bioturbated red marlstone and thin-bedded silt turbidites, Ypresian (NP11), creek 4.

3/20), *Cyclagelosphaera reinhardtii* (Fig. 3/22), *Eiffellithus turri-seiffeli*, *Micula staurophora*, *Prediscosphaera cretacea*, *Reticapsa crenulata*, and *Watznaueria barnesae* occur. At the top of the red marlstone outcrop, small specimens of *Ceratolithoides aff kamptneri* were observed (Fig.3/21), indicating already Zone CC26.

Two samples for foraminifera studies were taken from the red marlstone at the outcrop in creek 3 outcrop. The assemblages consist essentially of a rich agglutinated fauna and a

small number of calcareous benthic species. Very small planktic species were found only in one sample and display excellent grain-size sorting suggesting reworking by current activity.

The red marlstone transitionally passes into ca. 5 m of grey marlstone with intercalated thin carbonate-cemented parallel-laminated turbiditic siltstone and sandstone beds (Fig. 4). The best outcrop of these rocks was found in creek 2 about 10 m south of the hiking trail. In the lower part of this outcrop, carbonate values of three samples (TS2/09, TS7/09 and TS9/09)

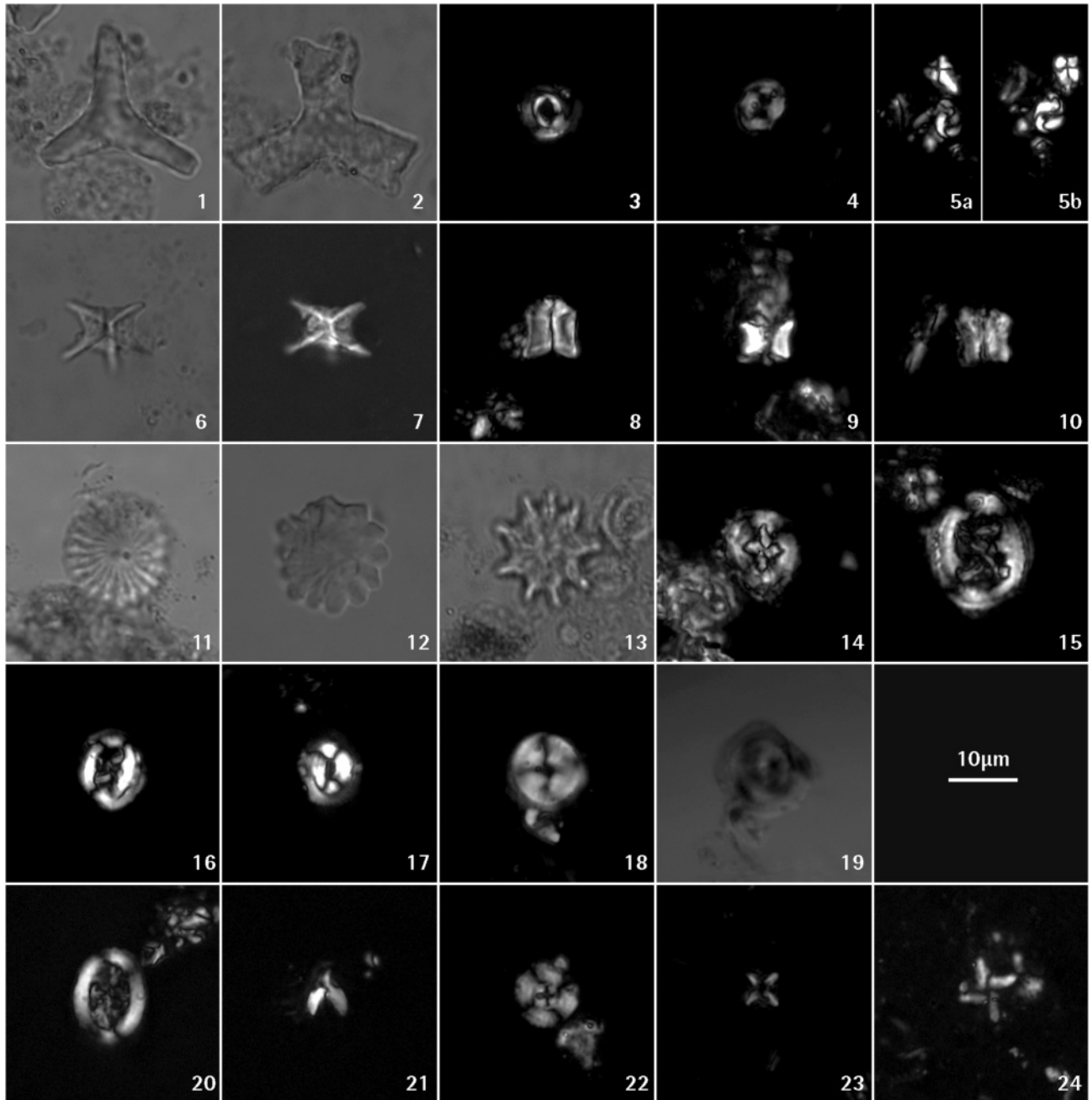


FIGURE 3: Calcareous nannoplankton from the Goppling section. Paleogene species: 1) *Tribrachiatus orthostylus* - Gstetten18/09; 2) *Tribrachiatus digitalis* - Gstetten10/09; 3) *Toweius callosus* - Gstetten22/09; 4) *Toweius occultatus* - Gstetten22/09; 5 a and b) *Sphenolithus anarrhopus* - Achthal 12/09; 6 and 7) *Rhombosaster cuspis* - Gstetten22/09; 8) *Fasciculithus tympaniformis* - Achthal12/09; 9) *Fasciculithus billii* - Achthal28/09; 10) *Fasciculithus ulii* - Achthal28/09; 11) *Discoaster multiradiatus* - Gstetten13/09; 12) *Discoaster mohleri* - Achthal12/09; 13) *Discoaster falcatus* - Gstetten13/09; 14) *Cruciplacolithus tenuis* - Achthal12/09; 15) *Chiasmolithus bidens* - Achthal12/09; 16) *Chiasmolithus danicus* - Achthal12/09; 17) *Coccolithus pelagicus* - Achthal12/09; 18 and 19) *Bomolithus elegans* - Achthal28/09. Maastrichtian: 20) *Arkhangelskiella cymbiformis* - Achthal18/09; 21) *Ceratolithoides aff kamptneri* - Achthal18/09; 22) *Cyclagelosphaera reinhardtii* - Achthal18/09; 23) *Micula staurophora* - TS10/09; 24) *Micula prinsii* - TS10/09.

range between 20.8 wt% and 21.5 wt%. In the upper part carbonate values decrease to 9.4 wt% (TS10/09) and finally to less than 2 wt% (TS12/09, TS13/09 and TS14/09). This change in the composition of pelitic rocks is interpreted as a shift of the depositional area to below the calcite compensation depth (CCD).

In the grey marlstone (TS1/09), *Micula prinsii* (Fig. 3/24) has its first occurrence. This species is indicative for the *Nephrolithus frequens* Zone (CC26), the youngest calcareous nannoplankton zone of the Maastrichtian. Consistent with the nannoplankton data, the dinoflagellate assemblages (Tab. 1) of six samples (TS4/09 to TS14/09) indicate a late Maastrichtian age of the grey marlstone and the claystone. *Disphaerogena carpospaeropsis* (TS8/09) had its first appearance in the latest Maastrichtian (e.g. Brinkhuis and Zachariasse, 1988; Moshkovitz and Habib, 1993; Habib, 1994; Nohr-Hansen and Dam, 1997), whereas *Dinogymnium acuminatum* (Fig. 5/1), which occurs in the claystone of the highest sample (TS14/09), does not cross the K/Pg-boundary (e.g. Stover et al., 1996).

4.2 DANIAN

Danian and Selandian deposits are almost continuously exposed in the Goppling creek gully. Due to the carbonate depletion, no calcareous plankton could be found in the siliciclastic succession, although dinoflagellate assemblages of samples Ach1/09 and Ach2/09 (see Tab. 1 and Fig. 6/6, 8 and 9) contain *Carpatella cornuta*, *Damassadinium californicum* and *Senoniasphaera inornata*, which have their first appearance date in the early Danian. *Palynodinium grallator* (Fig. 5/5 and 6) has its highest occurrence in the lowermost Danian planktonic foraminiferal Zone P1a (Habib et al., 1996; Dam et al., 1998; Brinkhuis et al., 1998). The samples were taken at the base (Ach1/09) and top (Ach2/09) of the same outcrop (Fig. 2/2). Consequently, this outcrop can be assigned to Zone P1a in the zonation of Berggren et al. (1995).

The Danian shows a two-fold lithological subdivision. The 30 m thick lower part is dominated by thin-bedded (< 40 cm) parallel-laminated sandstone turbidites, that rarely show thin capping mudstone (Fig. 2/2). In contrast to the Maastrichtian turbidites, the Danian ones

are not calcite cemented and do not contain carbonate at all. They are fine-grained (grain diameters up to 0.2 mm), show clast supported fabrics, and have a quartzarenitic composition (Fig. 7a). Beside quartz (ca. 90 % of the grains), feldspar, chert and glauconite occur as components. Freimoser (1972) noted that the heavy mineral assemblages of these Paleocene sandstones are essentially composed of zircon, tourmaline and rutile (together about 90 % of the assemblage). Hemipelagic claystone between the turbidite beds is rare and when present only a few millimeters thick indicating that (1) turbidity currents entered the basin with a high frequency and (2) deposition took place below the local CCD.

In the 40 m thick upper part of the Danian, hemipelagic layers are common and often display red colors (Fig. 2/3 and 4). Packages of red hemipelagic claystone contain thin base trun-

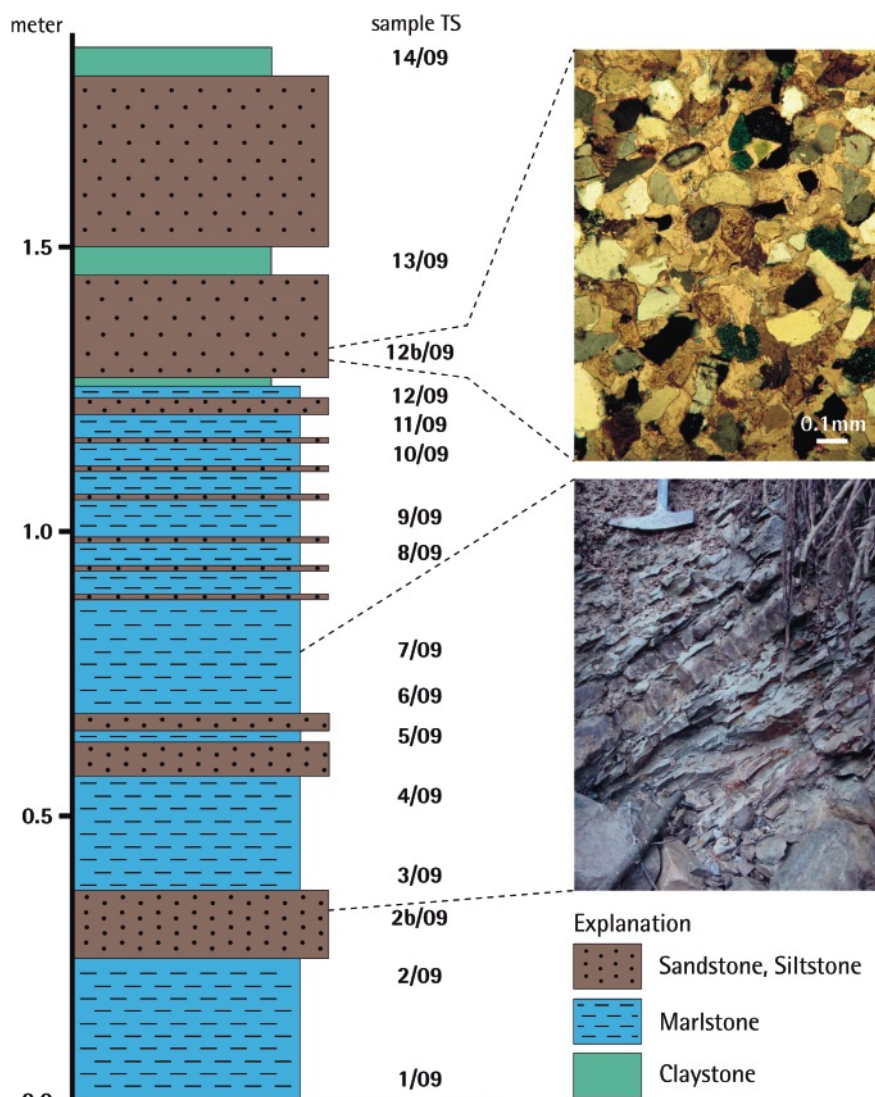


FIGURE 4: Log of the Upper Maastrichtian (*Micula prinsii*-Zone) in the creek 2 section. The lower photograph shows grey to pale red marlstone displaying carbonate contents of ca. 20wt% and intervening calcite cemented fine-grained turbiditic sandstone beds. The upper photograph is the image of a thin-section of such a sandstone. Calcite replacement affected the components (predominantly single-crystal quartz grains displaying straight extinction, small amounts of K-feldspar and glauconite, very rare mica and cherts) and a possible matrix. The composition of the original sandy fraction cannot be assessed due to the strong diagenetic alteration.

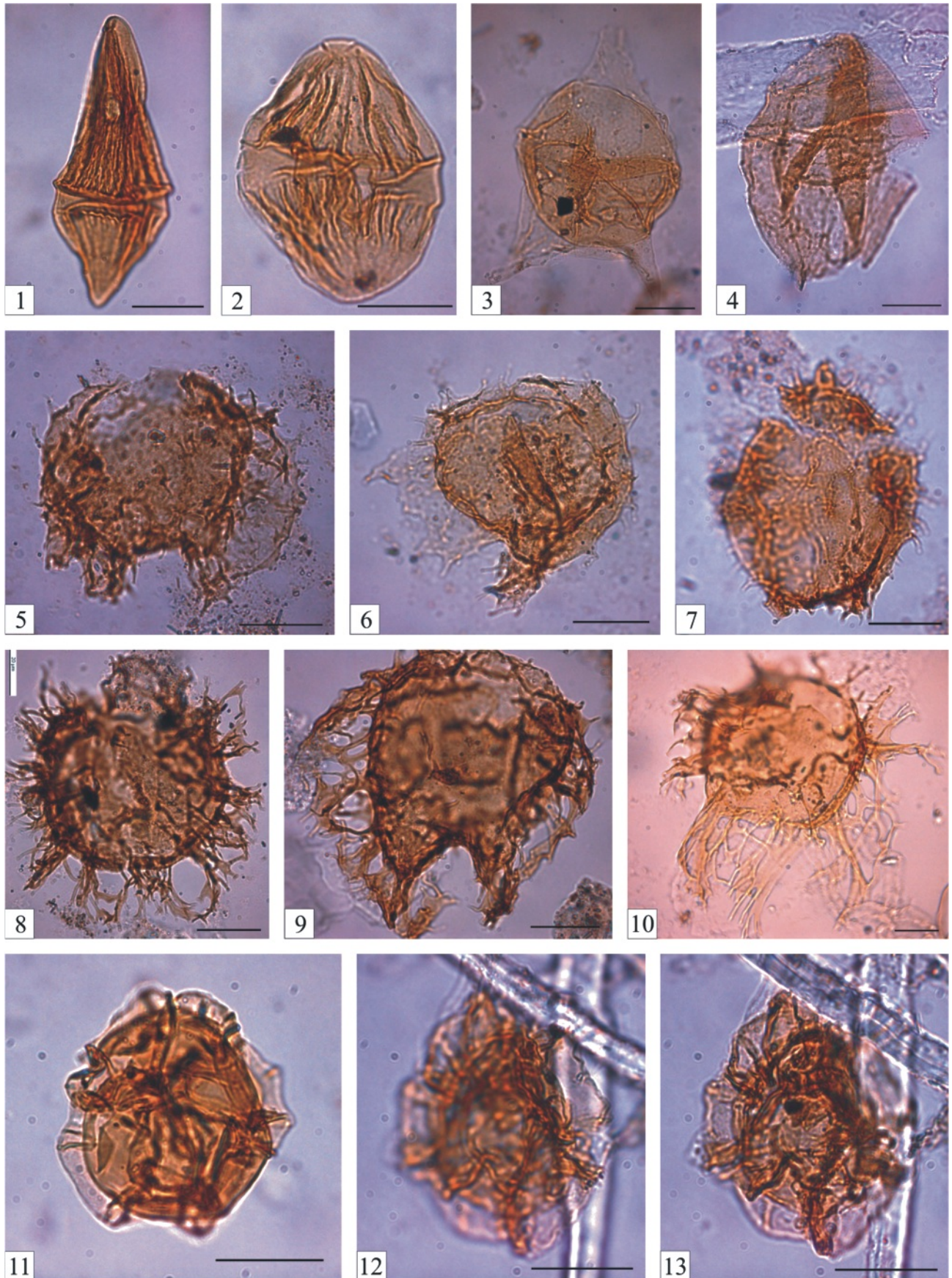


FIGURE 5: Dinoflagellate taxa from the Goppling section. The species name is followed by sample location and England Finder coordinates (for localization of the specimen on the slide). Scale is 20 μm . 1) *Dinogymnium acuminatum* - TS11/09/a, O24; 2) *Dinogymnium* sp. - TS11/09/a, F7/3; 3) *Cerodinium* sp. - TS11/09/a, X16/3; 4) *Trithyrodinium suspectum* - TS8/09/a, B24/2; 5) *Palynodinium grillator* - TS13/09/a, C40; 6) *Palynodinium grillator* - TS11/09/a, W36; 7) *Palynodinium minus* - TS13/09/b, Y27; 8) *Areoligera volata* - Ach.2/09/a, G12; 9) *Areoligera coronata* - Ach.1/09/a, A3; 10) *Areoligera gippingensis* - TS11/09/a, X34; 11) *Pterodinium cingulatum* subsp. *cingulatum* - TS12/09/a, W33/4; 12 and 13) *Pterodinium aliferum* - TS8/09/a, D6/1.

cated turbiditic siltstone to sandstone beds. These packages are separated by single thick (>0.5 m) medium to coarse-grai-

ned sandstone beds (Fig. 7b) showing grain diameters up to 1.0 mm. As in the lower Danian, only K-feldspar components

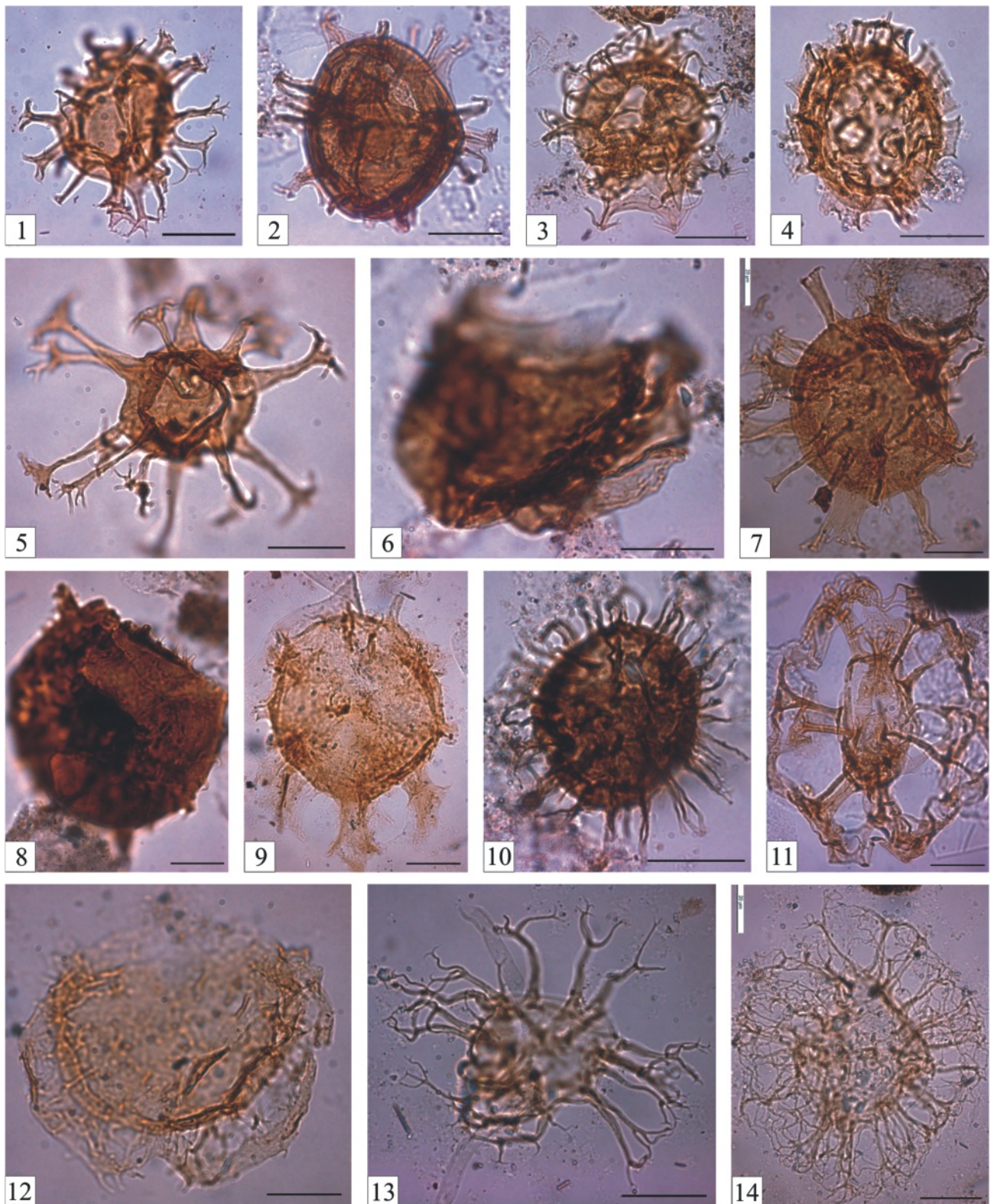


FIGURE 6: Dinoflagellate taxa from the Goppling section (continuation). The species name is followed by sample location and England Finder coordinates (for localization of the specimen on the slide). Scale is 20 μ m. 1) *Achomosphaera* cf. *alcicornu* - TS13/09/b, N5; 2) *Spiniferites pseudofurcatus* - TS4/09/b, X51/1; 3) *Hystrichostrogylon membraniphorum* - TS12/09/a, N24/2; 4) *Achilleodinium biformoides* - TS11/09/a, X8; 5) *Oligosphaeridium complex* - Ach. 2/09/a, G12; 6) *Senoniasphaera inornata* - Ach. 2/09/b, F40; 7) *Cordosphaeridium fibrospinosum* - TS12/09/a, B36/3; 8) *Carpatella cornuta* - Ach.1/09/b, K16; 9) *Damassadinium californicum* - TS11/09/a, P10; 10) *Operculodinium centrocarpum* - Ach.2/09/b, B25/4; 11) *Rigaudella aemula* - TS4/09/b, D18/1; 12) *Glaphyrocysta perforate* - TS11/09/a, S14/1; 13) *Surculosphaeridium longifurcatum* - TS11/09/a, M46/2; 14) *Trabeculidium quinquetrum* - TS12/09/a, D34/2.

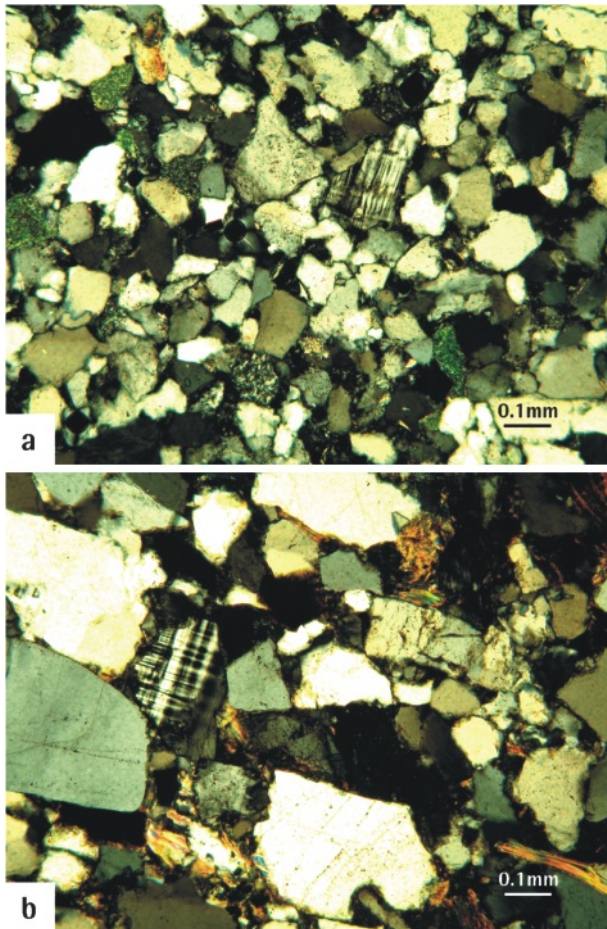


FIGURE 7: a) Image of a thin-section under cross-polarized light of a lower Danian thin-bedded sandstone (creek 3). b) Image of a thin-section under cross-polarized light of an upper Danian thick-bedded sandstone (creek 3).

can be observed and plagioclase is entirely absent. The beds are either massive or show stratification defined by 2-5 cm thick laminae. Graded (Ta) and parallel laminated (Tb) Bouma divisions form the major parts of these beds. Small-sized terrestrial plant remnants are commonly concentrated in horizontal Td-layers near the top of the beds and indicate a deriva-



FIGURE 8: Flute casts at the base of a south-dipping bed indicating longitudinal paleotransport from west to east (creek 3).

tion of the turbidite material from land areas. Submarine erosion is evidenced by flute casts, which indicate sediment transport predominantly from the west, parallel to the approximately east-west trending slope (Fig. 2/5).

One sample (Ach3/09) of the red claystone was studied for dinoflagellates but contained only *Areoligera senonensis*, which has a range from the Cretaceous to the Paleogene. Together with the last red hemipelagites, grey turbiditic clayey marlstones occur, containing strongly corroded nannoplankton assemblages. Beside substantial admixtures of Cretaceous species, *Chiasmolithus danicus*, *Cruciplacolithus tenuis*, *Coccolithus pelagicus* and *Toweius* spp. are indicative for the Danian (*Chiasmolithus danicus* Zone, NP3). However, the absence of *Ellipsolithus macellus*, the zonal marker for Zone NP4, might only be a consequence of the poor preservation in this sample.

4.3 SELANDIAN

About 10 m up-section from the above mentioned Danian sample, nannoplankton assemblages contain *Fasciculithus tympaniformis*, the zonal marker for the calcareous nannoplankton Zone NP5 of earliest Selandian age. With the disappearance of red hemipelagites the discrimination between turbiditic and non-turbiditic rocks becomes difficult. Single turbidites show a distinct pelitic component (Bouma T_d) in this part of the Goppling section, with approximately the same thickness as the sandy part of the turbidite. This turbiditic mudstone only occasionally contains carbonate. In most cases it is devoid of carbonate and displays the same grey color as the supposed hemipelagic mudstone.

The Selandian, which forms the morphologically steepest part in the course of creek 3, is composed of a ca. 25 m thick thickening and coarsening upward succession. In the lower part of this succession decimeter-scale turbidites occur. Continuing up the exposure, the bed thicknesses gradually increase up to 1.5 m at the top of the succession (Fig. 2/6). These sandstone beds are the thickest beds in the entire Achthal Formation and do not display turbiditic mudstone. In part, they contain intraformational mudstone clasts with diameters up to 0.2 m. Flute casts indicate paleotransport from west to east and thus an orientation parallel to the trend of the paleoslope (Fig. 8).

4.4 THANETIAN

In spite of excellent exposures along creek 3, the boundary between the Selandian and Thanetian is difficult to fix precisely due to carbonate depletion and the lack of calcareous plankton. Ca. 20 m downstream from the confluence in the uppermost part of creek 3 (Fig. 1), *Fasciculithus billii* is indicative for the upper part of Zone NP5. From here on upstream, a ca. 40 m thick part of the section is characterized by abundant olive-green strongly bioturbated „spotty“ claystone. Probably, the majority of the oval spots in these hemipelagic deposits represent cross sections of the trace fossils *Planolites* and *Thalassinoides* (Uchman, 1999). *Thalassinoides* ispp. and a strongly fragmented specimen of ?*Scolica strozzii* were found also as semi-reliefs at the base of turbidite beds (Fig. 9/4, 5 and 6).

The turbidites intervening with the claystone are mostly thin bedded and occasionally display substantial amounts of glauconite, resulting in green rock colors. Glauconite was deformed during burial and flowed around adjacent quartz grains. This is indicated by the patchy distribution of glauconite-filled areas, which are much larger than normal pores (Fig. 10).

Some beds show a lenticular shape. The orientation of paleoflow indicators (flute casts and erosional channels) suggest

paleotransport from north to south, following the gradient of the south-facing paleoslope (Fig. 2/7 and Fig. 11). *Discoaster mohleri* (Fig. 3/12) indicative of Thanetian zone NP7, was found in the eastern branch of creek 3, about 50 m up-stream from the confluence with the western branch (Fig. 1). *Discoaster multiradiatus* (Fig. 3/11), the zonal marker of Zone NP9, was found in the uppermost part of the western branch.

The following 100 m of section are only poorly exposed in

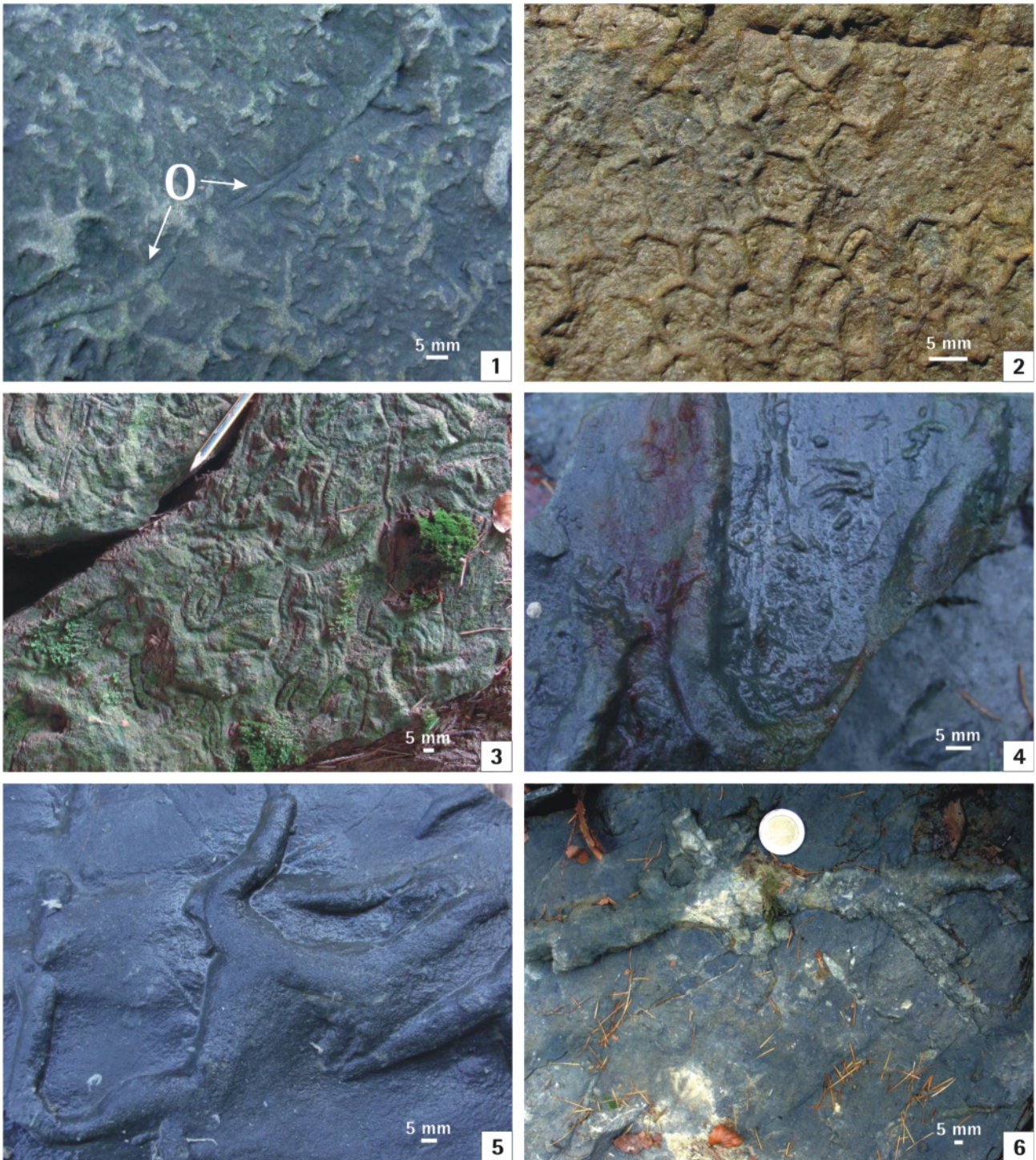


FIGURE 9: Ichnofossils from the Thanetian (creek 3) and Ypresian (creek 4) of the Goppling section 1) *Ophiomorpha annulata* (O) and ? *Protopaleodictyon* isp. - creek 3; 2) *Paleodictyon majus*.- creek 4; 3) *Scolicia prisca* - creek 4; 4) ?*Scolicia strozzii* - creek 3; 5) *Thalassinoides* isp. - creek 3; 6) *Thalassinoides* isp. – creek 3.

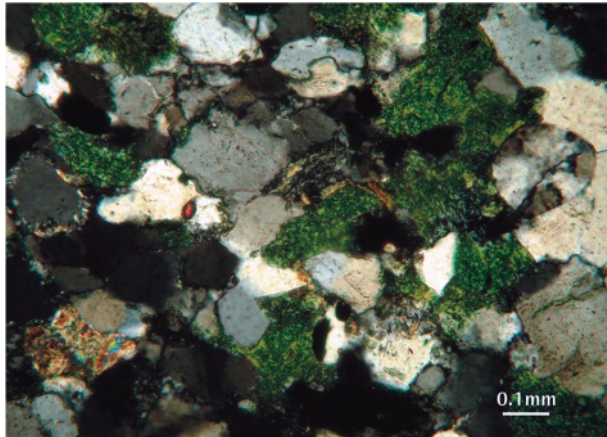


FIGURE 10: Image of a thin-section under cross-polarized light from a Thanetian sandstone rich in glauconite (creek 3).

the two small gullies (without numbers in Fig. 1) east of the creek 3. Only minor outcrops of a carbonate depleted facies occur and these provided no calcareous plankton. It is assumed that these outcrops are still in the Paleocene part of Zone NP9.

4.5 YPRESIAN

The Ypresian of the Goppling section shows a two-fold lithological subdivision. The lower part consists of a ca. 50 m thick succession of decimeter-scale turbiditic sandstone and siltstone beds alternating with red colored marly claystone (Fig. 2/8). The latter rock is often bioturbated and probably represents hemipelagic non-turbiditic material. As its carbonate values range between 4 wt% and 8 wt%, sedimentation slightly above the CCD can be assumed.

Samples containing *Rhomboaster cuspis* (Fig. 3/4 and 5) were found in the lower part of creek 5, about 20 m to the north of the hiking trail. *R. cuspis* has its first appearance date at the Paleocene/Eocene-boundary, which is situated in the upper third of Zone NP9. About 25 m to the south of the hiking trail, *Tribrachiatius digitalis* (Fig. 3/2) occurs, the marker fossil of sub-Zone NP10b in the refined zonation scheme of Aubry (1992). About 15 m further up-section, another outcrop of the red bed



FIGURE 11: Flute casts at the base of a south-dipping bed indicating transversal paleotransport from north to south (creek 3).

facies occurs and provided *Tribrachiatius orthostylus* (Fig. 3/1), whereas *T. contortus*, which has its highest occurrence at the NP10/NP11-boundary is absent. Therefore these samples can be assigned to the lower part of NP11 (*Discoaster binodosus*-Zone). Thus, in summary, the red bed facies encompasses the upper part of NP9 to the lower part of NP11.

Along strike to west, red beds containing *R. cuspis* were found in the upper part of creek 4. These deposits are separated by a fault from the underlying part of the succession in creek 4. In this gully, the topographically lowest outcrops lie just downstream the hiking trail (Fig. 2/8). *T. orthostylus* with pointed rays (Fig. 3/1) co-occurs with *Chiasmolithus bidens*, *Coccolithus pelagicus*, *Discoaster barbadiensis*, *D. multiradiatus*, *Ellipsolithus macellus* and *Sphenolithus primus*. Whereas the robust and dissolution resistant *Tribrachiatius* specimens may be common in the samples, the other species, in particular the discoasterids, are exceedingly rare due to dissolution. Carbonate values of two samples from this outcrop were 4.2 wt% and 4.8 wt%.

A few meters up-stream from the hiking trail the red bed facies in creek 4 shows a sharp sedimentary contact to an overlying ca. 60 m thick sand-rich and thin-bedded turbidite succession that displays only rare and very thin carbonate depleted hemipelagic layers (Fig. 12). This suggests that the upper part of the Ypresian succession was deposited below the CCD and hence another subsidence pulse can be assumed. This interpretation is supported by the orientation of flute casts, which indicate paleoflow directions from west to east.

This part of the Goppling section commonly contains trace fossils (e.g. *Paleodictyon majus* and *Scolicia prisca*, see Fig. 9/2 and 3). According to Uchman (1999) the ichnogenus *Paleodictyon* probably reflects a moderate shortage of food. These generally oligotrophic conditions were interrupted by periodic accumulation of organic detritus (e.g. plant detritus) by turbidity currents. These more eutrophic episodes favored the ichnogenera *Ophiomorpha* and *Scolicia*. In the Rhenodanubian Group (Egger and Schwerd, 2008) of the adjacent abyssal Penninic basin, the ichnogenera *Ophiomorpha*, *Paleodictyon* and *Scolicia* are known exclusively from the Greifenstein Formation of Eocene age (Uchman, 1999).

5. DEPOSITIONAL EVOLUTION

Predominant dissolution-resistant species in the calcareous nannoplankton assemblages and the composition of foraminifera assemblages indicate sedimentation of the Maastrichtian red clayey marlstone in a deep-water environment. The absence of an autochthonous planktic fauna indicates deposition below the foraminiferal lysocline, where all planktic foraminifera are dissolved (Berger, 1970). Below the lysocline and above the calcite compensation depth (CCD) calcareous nannoplankton form coccolith ooze, because in spite of their small size, some coccoliths are more dissolution-resistant than foraminifera (see Hay, 2004, for a review).

In the shallower parts of the Ultrahelvetic slope, Cretaceous oceanic red beds (CORBS) occur from the Middle Turonian

up to the Lower Campanian (Wagreich et al., 2009). Within in the Lower Campanian, the red color fades out and light-gray marlstones (carbonate values >45 wt%) become the dominant rock type. The red color in the Maastrichtian of the Goppling section indicates that an increase in paleowater depth favors the formation of CORBS, probably as an effect of decreased sedimentation rates due to increased carbonate dissolution.

In the latest Maastrichtian, rapid subsidence brought the Ultrahelvetetic sea-floor to below the CCD. Associated with this regional subsidence along the southern continental margin of the European Plate, was the onset of turbidite sedimentation (Fig. 13). Turbidity currents running parallel with the strike of the slope indicate an opposing topographic high, which caused deflection of the down slope sediment transport (Kneller and McCaffrey, 1999). Subsidence of the sea-floor associated with the deposition of sediment-gravity flows and the coeval generation of a sea-ward bounding topographic high suggest the formation of an intra-slope basin on subsiding crustal fault blocks.

Due to the lack of information about the three-dimensional geometry of the basin-fill, the scale and shape of this basin is unknown. It can be assumed that it was a narrow elongate, structurally controlled depression where tectonic activity was the primary control on sedimentation. Presumably, this confined basin was too small for the development of a large-scale deep-sea fan. Instead a channelized deep-water system could be expected, with the bounding slopes of the basin acting as channel walls. Gravity-induced flows entering a sub-basin drop

their sediment load and prograde across the depression forming a thickening and coarsening upward succession (Anderson et al., 2006; Shultz and Hubbard, 2005).

At the front of this prograding lobe-like body the thin-bedded sand-rich turbidite succession of early Danian age was deposited (e.g. Crabaugh and Steel, 2004). The lack of muddy tops can be interpreted as an effect of flow-stripping of the fine-grained component of the turbidity currents (e.g. Piper and Normark, 1983; Sinclair and Tomasso, 2002). This indicates that during this early stage of basin evolution, the confining sill was still low. Hence it could be surmounted by the lower-density fraction of the turbidity currents, while the coarse-grained higher density portions of the flows were deflected and preserved upstream of the barrier. The rare and thin hemipelagites indicate the existence of high-frequency trigger mechanisms (e.g. earthquakes) for turbidity currents during the onset of basin formation.

In a conventional fan model, the upper Danian packages of thin-bedded turbidites and red hemipelagic mudstone, which are separated by single thick sandstone beds, can be interpreted as interchannel deposits. In such a model, the thin-bedded turbidites are thought to result from low-density currents overflowing adjacent active channels, while the thicker beds are explained as the result of crevasses in the channel levee, which let high density turbidity currents (Lowe, 1982) escape to the basin floor (e.g. Mutti, 1977). This model implies the existence of subordinate fairways within the slope-basin.

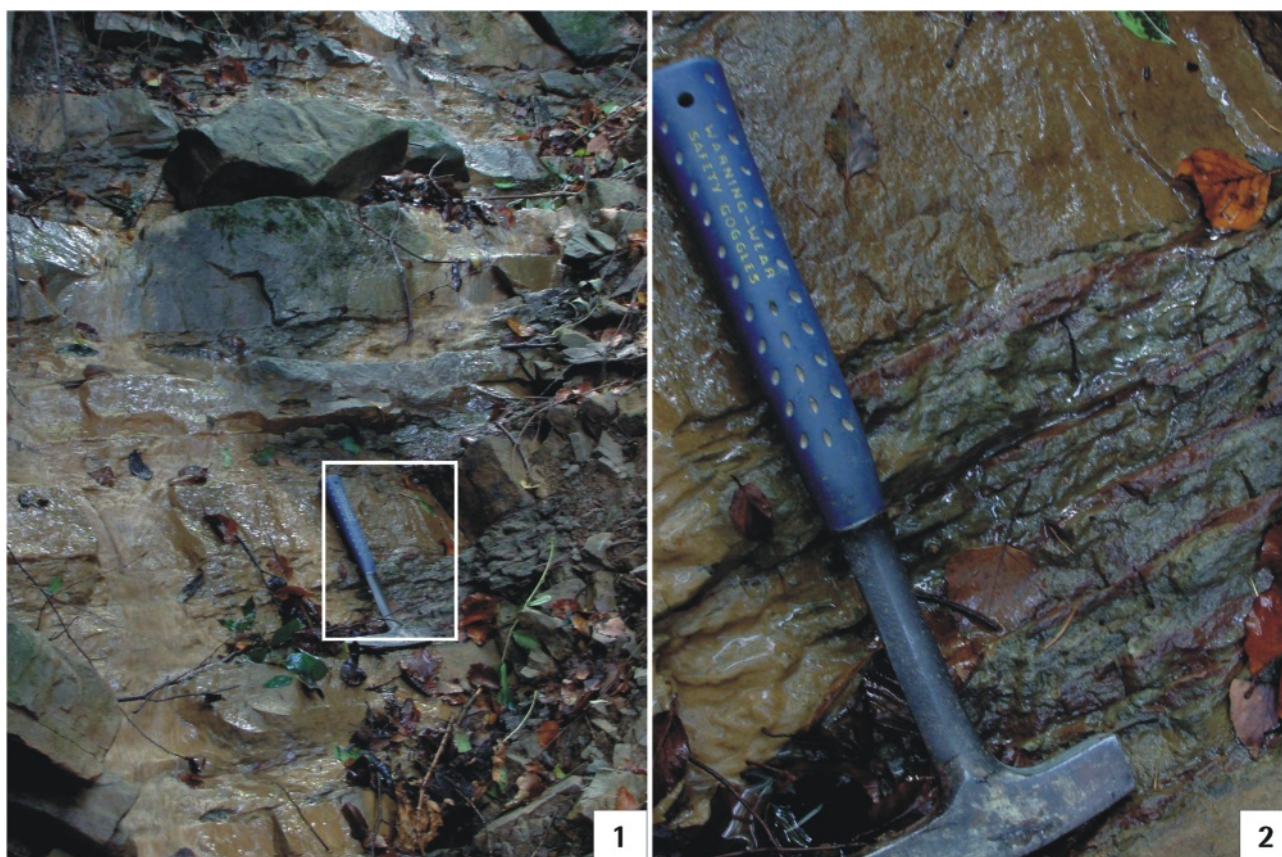


FIGURE 12: The Ypresian sand-rich turbidite succession and intercalated red hemipelagic claystone in creek 4.

Alternatively, the upper Danian facies can be seen as the result of an episode of comparatively tectonic quiescence. Siliciclastic material accumulated at the shelf edge over time and larger turbidity currents triggered by earthquakes or gravity load entered the slope-basin with low periodicity. This is indicated by the common occurrence of intervening hemipelagic red claystone as their deposition indicates very low sedimentation rates. The lack of muddy tops of the thick-bedded turbidites can again be explained as a result of flow-stripping as flow thickness was determined as the primary control of the run-up distance of a turbidity current onto the opposing slope (Muck and Underwood, 1990). It is assumed, that high-density currents (Lowe, 1982) lost their fine-grained component by down-spill, so that only their coarse-grained material is preserved in the sub-basin. Low-density currents had not the potential to surmount the bounding slope and remained completely in the sub-basin.

Increased subsidence at the end of the Danian caused ponding of the turbidity currents, which display a distinct pelitic component. However, sedimentation rates quickly outpaced subsidence rates and deposition reduced the relief sufficiently to allow spill down-slope. The filling up of the basin to the spill-point is indicated by downslope paleotransport directions in the upper Selandian and Thanetian. Due to the gradient reduction in the area of the former basinal structure turbidites were deposited on this flat surface and the ca. 95 m thick basin-fill succession of Danian and Selandian age became buried by slope deposits developing into a healed slope (e.g. Smith, 2004).

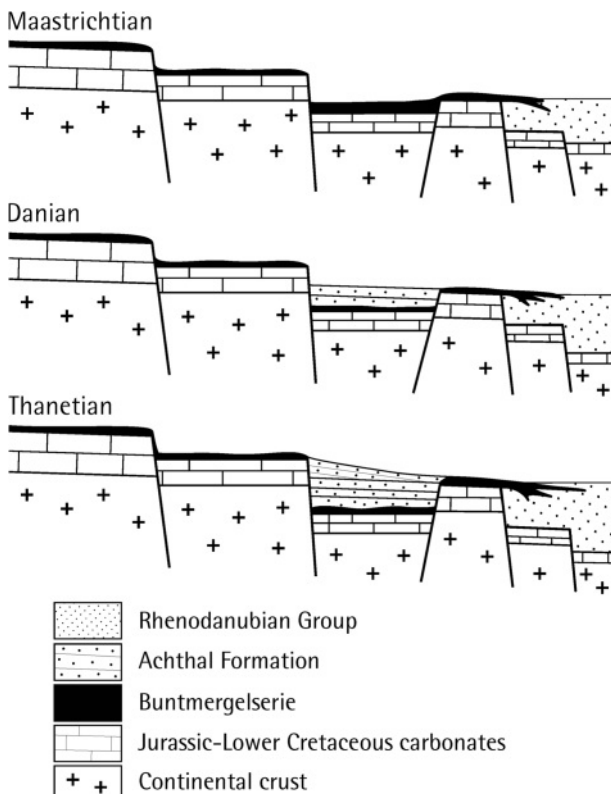


FIGURE 13: Slope basin model for the deposition of the Achthal Formation.

On a global scale, the CCD shoaled rapidly by more than two kilometers and recovered gradually at the Paleocene/Eocene-boundary (Egger et al., 2005; Zachos et al., 2005). The carbonate contents of the Ypresian red beds in the Goppling section indicate that the level of the CCD after the recovering phase following the Paleocene/Eocene-boundary was deeper than before this event. Subsequently, renewed subsidence changed the slope topography and formed a new depression with a floor below the CCD. This structure was filled up by sand-rich turbidity currents running parallel to the strike of the slope. Due to the lack of calcareous plankton, it remains unclear if this part of the section still represents Zone NP11 or reaches up into Zone NP12 (*Discoaster lodoensis*-Zone).

6. LITHOSTRATIGRAPHIC DEFINITION OF THE ACHTHAL FORMATION

The name Achthal Formation is proposed for the above described and interpreted 320 m thick deep-water system of latest Maastrichtian to Ypresian age (Fig. 14). The lithostratigraphic term "Achthaler Sandstein" dates back to Gümbel (1862, p.616). Although Schlosser (1925, p.167) mentioned a Thanetian macrofauna from this unit ("Achthaler Grünsand"), it can be assumed that these fossils originated from the tectonically neighbouring shallow-water deposits of the south-Helvetic thrust unit. Ganss and Knipscheer (1956) report on Paleocene foraminifera faunas and interpreted the outcrops as a special facies (Teisendorf facies) of the Helvetic sedimentation area. Hagn (1960 and 1967) recognized the deep-water character of the deposits and assigned them to the southern part of the Ultrahelvetic sedimentation area, which interpretation is adopted in this paper.

The type area of the Achthal Formation is the forest ("Stecherwald") southwest of Teisendorf. The base of the composite type section of the Achthal Formation (Goppling section) is located in creek 3 ("Gopplingbach"), ca. 15 m south of the hiking trail bridge (coord. E 012° 47' 42", N 47° 50' 51"). Further up-stream the Danian, Selandian and lower Thanetian all show excellent exposures, which end at the hamlet of Goppling. The upper Thanetian is seen only in small and poor exposures, in the two gullies east of creek 3 (Fig. 1). The Eocene part of the section is well exposed along creek 4, with the first outcrop ca. 20 m downstream from the hiking trail (coord. E 012° 48' 02", N 47° 50' 48").

The base of the Achthal Formation, which conformably overlies the Buntmergelserie, is defined by the onset of turbiditic sedimentation in the uppermost Maastrichtian. The stratigraphic top is unknown because of the tectonic truncation of the Goppling section. However, deposition of the Achthal Formation probably ended in the Ypresian because grey calcareous marlstone of early Lutetian age occurs in the Ultrahelvetic thrust unit at Mattsee in Austria (Rögl and Egger, 2010), only ca. 25 km northeast of Teisendorf.

7. DISCUSSION

Sedimentary successions rich in turbidites other the Achthal

Formation, are known from a number of Ultrahelvetetic sites. In Vorarlberg, grey turbidites and hemipelagic marlstone (Kehlegg beds) were assigned to the Ultrahelvetetic unit by Oberhauser (1991). The base of the Kehlegg beds is situated around the K/Pg-boundary. The unit comprises the entire Paleocene (Egger, unpublished) and its top is tectonically truncated by an overthrust. In a more southerly paleogeographic position on the slope, the deep-water system of the Feuerstätt thrust unit was deposited, exposed in Vorarlberg and southwestern Germany (see Schwerd and Risch, 1983 for a review). There, turbidites and intervening red claystone ("Rote Gschlief-Schichten") of Paleocene and Early Eocene age may represent the in-fills of adjacent slope basins at different paleodepths on the continental slope (Weidich and Schwerd, 1987; Schwerd, 1996). Farther to the east, in Lower Austria, Paleocene to Eocene turbidite successions associated with Buntmergelserie are reported by Prey (1957).

In summary, the style of early Paleogene turbidite sedimentation on the European continental margin seen at the Goppling section was not a unique phenomenon. Rather, it occurred at several sites along the strike of the Ultrahelvetic thrust unit in the Eastern Alps. Although it is unlikely that these deposits originated from the same basin. Instead, a number of small sub-basins can be assumed, which due to the different subsidence histories and their different bathymetric positions, probably cannot be directly correlated. More realistically, each basin-fill has to be considered as its own lithostratigraphic unit.

The largely synchronous formation of different sub-basins along the strike of the Ultrahelvetic slope points to large-scale tectonic deformation of the continental margin, starting in the Late Maastrichtian. The subsidence of intra-slope basins can be related to an extensional tectonic regime. However, for the same period, Nachtmann and Wagner (1987), Wessely (1987), and Ziegler (2002) all document strong intra-plate compressional deformation of the foreland of the Eastern Alps. Together with the data from the Goppling section and other Ultrahelvetic sites, this implies that the southern European plate was simultaneously affected by extension and compression. Here, this style of deformation is typical for anastomosing strike-slip fault zones in convergent settings (e.g. Crowell, 1974).

The well-established contractional deformation event, which affected the European plate in Late Cretaceous times, was explained by two different models. In the first one, strike-

slip faulting was driven by the oblique convergence of the European and African plates resulting in a dextral transpressional tectonic regime subsequently to the onset of the collision (Ziegler, 1987). In the second model, this deformation is seen as the result of an important change in relative motion between the European and African plates causing pinching of Europe's lithosphere between Africa and Baltica (Kley and Voigt, 2008). This model explains better than the collision model the uniform N to NE intraplate shortening of the European plate during the Late Cretaceous event and is also consistent with the NE-SW trending strike-slip faults, which affected the European margin and led to the formation of slope-basins.

Syn depositional faulting and the associated alteration in margin topography, changed sediment dispersal and accumulation not only on the slope but also in the adjacent Penninic basin. There, a dearth of turbidite sedimentation (=Strubach-Tonstein, Egger, 1995) has been recognized in the Paleocene of the Rhodanubian Group. This was interpreted to be the result tectonic activity, that caused a cut-off of the basin from its source areas (Egger et al., 2002). More precisely, the data presented here suggest that structurally controlled slope-basins acted as sediment traps and prevented turbidity current by-pass to the main basin.

The above mentioned turbidite successions of Ultrahelvetic origin differ in age from the "Ultrahelvetic Flysch" of the Western Alps in Switzerland. This lithostratigraphic term is assign-

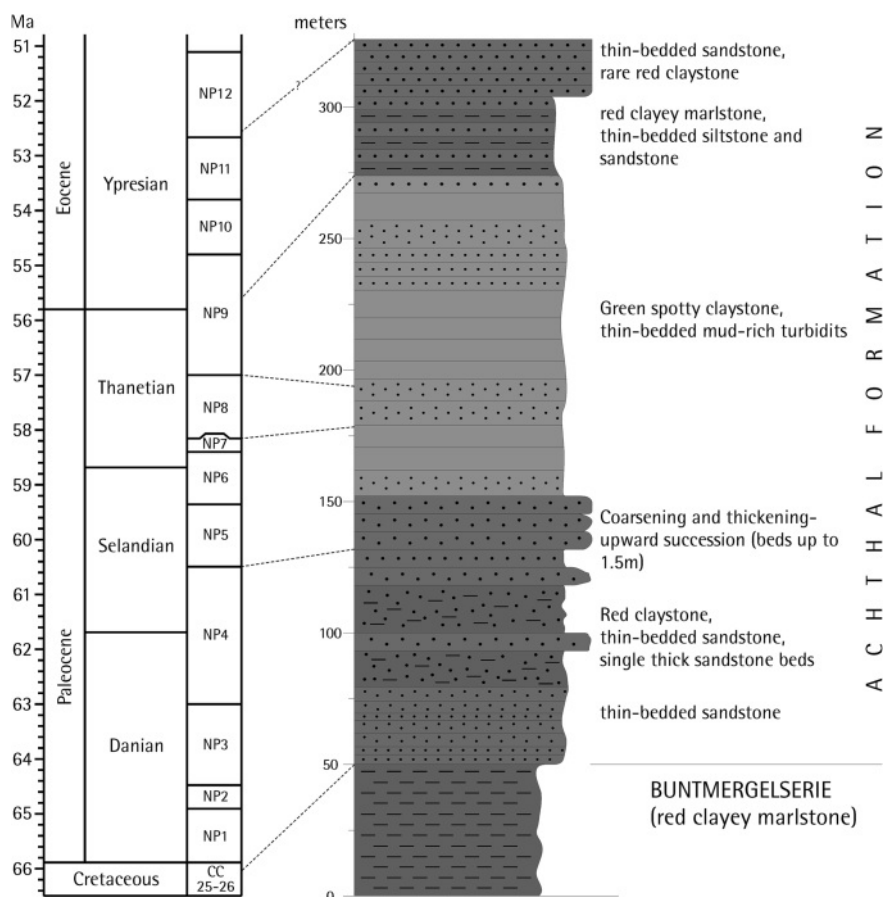


FIGURE 14: Composite log of the Achthal Formation in the type area (Stecherwald near Teisendorf).

ned to Middle to Upper Eocene turbidite successions, that occur as tectonic slices between the main Helvetic and Penninic thrust units (Homewood, 1977). These deposits are definitely younger than the Ultrahelvetetic deep-sea systems in the Eastern Alps.

8. CONCLUSIONS

The deep-water system of the Achthal Formation is interpreted to have initially filled a slope depression lying above a subsiding basement fault block. Initial subsidence occurred in the latest Maastrichtian and continued into the early Paleogene. Synsedimentary tectonic activity was the primary control on the depositional evolution of the slope-basin. The sedimentary records of different sites along the strike of the Ultrahelvetetic continental margin suggest that several such sub-basins existed at about the same time. These basins acted as sediment traps and thus controlled sedimentation in the adjoining Penninic basin.

ACKNOWLEDGEMENTS

We are indebted to Gerhard Hobiger (Vienna) for carbonate analyses of marlstones, to Fred Rögl (Vienna) for information on foraminifera assemblages, to Klaus Schwerd (Munich) for information on the regional geology and to Alfred Uchman (Krakow) for the determination of ichnofossil species. We thank Hugh Rice for improving the English of the original manuscript and Markus Kogler for preparing the figures. Constructive and helpful reviews by Pi Suhr Willumsen (University of Lund) and Michael Wagneich (Vienna University) are gratefully acknowledged.

REFERENCES

- Anderson, K.S., Graham, S.A. and Hubbard, S.M., 2006. Facies, architecture, and origin of a reservoir-scale sand-rich succession within submarine canyon fill: insights from Wagon Caves Rock (Paleocene), Santa Lucia Range, California, U.S.A. *Journal of Sedimentary Research* 76, 819-838.
- Aubry, M.-P., 1992. Towards an Upper Paleocene - Lower Eocene high resolution stratigraphy based on calcareous nannofossil stratigraphy. *Israel Journal of Earth Sciences* 44, 239-253.
- Berger, W.H., 1970. Planktonic foraminifera: selective solution and paleoclimatic interpretation. *Marine Geology* 8, 111-138.
- Berggren, W.A., Kent, D.V., Swisher, C.C., and Aubry, M.-P., 1995. A revised cenozoic geochronology and chronostratigraphy. *Society for Sedimentary Geology Special Publication* 54, 129-212.
- Brinkhuis, H. and Zachariasse, W.J., 1988. Dinoflagellate cysts, sea level changes and planktonic foraminifers across the Cretaceous-Tertiary boundary at El-Haria, Northwest Tunisia. *Marine Micropaleontology* 13, 153-191.
- Brinkhuis, H., Bujak, J.P. and Versteegh, G.J.M., Visscher, H., 1998. Dinoflagellate-based sea surface temperature reconstructions across the Cretaceous-Tertiary boundary. *Palaeogeography, Palaeoclimatology, Palaeoecology* 141, 67-83.
- Crabaugh, J.P. and Steel, R.J., 2004. Basin-floor fans of the Central Tertiary Basin, Spitsbergen: relationship of basin-floor sand-bodies to prograding clinoforms in a structural active basin. In: Lomas, S.A. and Joseph, P. (eds.): *Confined turbidite systems*. Geological Society, London, Special Publication 222, 187-208.
- Crowell, J.C., 1974. Origin of late Cenozoic basins in southern California. In: Dickinson, W.R. (ed.): *Tectonics and Sedimentation*. Society of Economic Paleontologists and Mineralogists Special Publication 22, 190-204.
- Dam, G., Nøhr-Hansean, H. and Kennedy, W. J., 1998. The northernmost marine Cretaceous-Tertiary boundary section: Nuussuaq, West Greenland. *Geology of Greenland Survey Bulletin* 180, 138-144.
- Egger, H., 1995. Die Lithostratigraphie der Altenglach-Formation und der Anthering-Formation im Rhenodanubischen Flysch (Ostalpen, Penninikum). *Neues Jahrbuch für Geologie und Paläontologie Abhandlungen* 196, 69-91.
- Egger, H., Homayoun, M. and Schnabel, W., 2002. Tectonic and climatic control of Paleogene sedimentation in the Rhenodanubian Flysch Basin (Eastern Alps, Austria). *Sedimentary Geology* 152, 247-262.
- Egger, H., Homayoun, M., Huber, H., Rögl, F. and Schmitz, B., 2005. Early Eocene climatic, volcanic, and biotic events in the northwestern Tethyan Untersberg section, Austria. *Palaeogeography, Palaeoclimatology, Palaeoecology* 217, 243-264.
- Egger, H. and Schwerd, K., 2008. Stratigraphy and sedimentation rates of Upper Cretaceous deep-water systems of the Rhenodanubian Group (Eastern Alps, Germany). *Cretaceous Research* 29, 405-416.
- Fensome, R.A., MacRae, R.A. and Williams, G.L., 2008. DINOFLAJ2, Version 1. American Association of Stratigraphic Palynologists, Data Series no. 1, 939 pp.
- Freimoser, M., 1972. Zur Stratigraphie, Sedimentpetrographie und Faziesentwicklung der Südostbayerischen Flyschzone und des Ultrahelvetikums zwischen Bergen / Obb. und Salzburg. *Geologica Bavarica* 66, 7-91.
- Ganss, O. and Knipscheer, H.C.G., 1956. Die Maastricht-Eozän-Folge des Helvetikums im Sprunggraben bei Oberteisendorf (Obb.) und ihre Gliederung mit Hilfe pelagischer Foraminiferen. *Geologisches Jahrbuch* 71, 617-630.
- Gümbel, C.W., 1862. *Geognostische Beschreibung des bayrischen Alpengebirges und seines Vorlandes*. 950 pp., Gotha (Justus Perthes).

- Habib, D., 1994. Biostratigraphic evidence of the KT boundary in the eastern Gulf coastal plain north of the Chicxulub Crater. *Lunar and Planetary Institute Contributions* 825, 45-46.
- Habib, D., Olsson, R.K., Liu, C. and Moshkovitz, S., 1996. High-resolution biostratigraphy of sea-level low, biotic extinction, and chaotic sedimentation of the Cretaceous-Tertiary boundary in Alabama, north of the Chicxulub crater. In: Ryder, G., Fastovsky, D. and Gartner, S. (Eds.), *The Cretaceous/Tertiary Event and Other Catastrophes in Earth history*. Geological Society of America, Special Paper 307, pp.243-252.
- Hagn, H., 1960. Die stratigraphischen, paläogeographischen und tektonischen Beziehungen zwischen Molasse und Helvetikum im östlichen Oberbayern. *Geologica Bavarica* 44, 5-208.
- Hagn, H., 1967. Das Alttertiär der Bayerischen Alpen und ihres Vorlandes. *Mitteilungen Bayerische Staatssammlung Paläontologie und historische Geologie* 7, 245-320.
- Hay, W.W., 2004. Carbonate fluxes and calcareous nannoplankton. In: Thierstein, H.R. and Young, J.R. (eds.): *Coccolithophores*, pp.509-528 (Springer).
- Homewood, P.W., 1977. Ultraschelvetic and North-Penninic Flysch of the Prealps: A general account. *Eclogae geologicae Helveticae* 70, 627-641.
- Kirsch, K.-H., 1991. Dinoflagellatenzysten aus der Oberkreide des Helvetikums und Nordultraschelvetikums von Oberbayern. - *Münchener Geowissenschaftliche Abhandlungen (A)* 22: 306 pp., Munich.
- Kley, J. and Voigt, T., 2008. Late Cretaceous intraplate thrusting in central Europe: Effect of Africa-Iberia-Europe convergence, not Alpine collision. *Geology* 36, 839-842.
- Kneller, B. and McCaffrey, W., 1999. Depositional effects of flow nonuniformity and stratification within turbidity currents approaching a bounding slope: deflection, reflection and facies variation. *Journal of Sedimentary Research* 69, 980-991.
- Kuhn, W. & Kirsch, K.-H., 1992. Ein Kreide/Tertiär-Grenzprofil aus dem Helvetikum nördlich von Salzburg (Österreich). *Mitteilungen Bayerische Staatssammlung für Paläontologie und historische Geologie* 32, 23-35.
- Lowe, D.R., 1982. Sediment gravity flows: II. Depositional models with special reference to the deposits of high-density turbidity currents. *Journal of Sedimentary Petrology* 52, 279-297.
- Martini, E., 1971. Standard Tertiary and Quaternary calcareous nannoplankton zonation. In: Farinacchi, A. (ed.): *Proceedings II Planktonic Conference Roma 1970/2*, pp.739-785.
- Moshkovitz, S. and Habib, D., 1993. Calcareous nannofossil and dinoflagellate stratigraphy of the Cretaceous-Tertiary boundary, Alabama and Georgia. *Micropaleontology* 39, 167-191.
- Muck, M.T. and Underwood, M.B., 1990. Upslope flow of turbidity currents: A comparison among field observations, theory, and laboratory models. *Geology* 18, 54-57.
- Mutti, E., 1977. Distinctive thin-bedded turbidite facies and related depositional environments in the Eocene Hecho Group (South-central Pyrenees, Spain). *Sedimentology* 24, 107-131.
- Nachtmann, W. and Wagner, L., 1987. Mesozoic and early Tertiary evolution of the Alpine foreland in Upper Austria and Salzburg, Austria. *Tectonophysics* 137, 61-76.
- Nøhr-Hansen, H. and Dam, G., 1997. Palynology and sedimentology across a new marine Cretaceous-Tertiary boundary section on Nuussuaq, West Greenland. *Geology* 25, 851-854.
- Oberhauser, R., 1991. Erläuterungen zur geologischen Karte der Republik Österreich 1 : 25.000 Blatt 110 St. Gallen Süd und 111 Dornbirn Süd. 72 pp., Vienna (Geologische Bundesanstalt).
- Piper, D.J.W. and Normark, W.R., 1983. Turbidite-deposits, patterns and flow characteristics, Navy Submarine Fan, California borderland. *Sedimentology* 30, 681-694.
- Prey, S., 1952. Aufnahmen in der Flyschzone auf den Blättern Gmunden-Schafberg (4851) und Kirchdorf/Krems (4852) (Gschliefgraben), sowie den Blättern Ybbs (4754) und Gaming-Mariazell (4854) (Rogatsboden).-*Verhandlungen der Geologischen Bundesanstalt* 1952, 41-45.
- Prey, S., 1953. Flysch, Klippenzone und Kalkalpenrand im Almtal bei Scharnstein und Grünau (OÖ.). *Jahrbuch der Geologischen Bundesanstalt* 100, 299-358.
- Prey, S., 1957. Ergebnisse der bisherigen Forschungen über das Molassefenster von Rogatsboden (NÖ.). *Jahrbuch der Geologischen Bundesanstalt* 100, 299-358.
- Rögl, F. and Egger, H., 2010. The missing link in the evolutionary origin of the foraminiferal genus *Hantkenina* and the problem of the lower-middle Eocene boundary. *Geology* 38, 23-26.
- Schlosser, M., 1925. Die Eocänfaunen der bayerischen Alpen. 1. Teil: Die Faunen des Unter- und Mitteleocän. *Abhandlungen Bayerische Akademie der Wissenschaften, Mathematisch-naturwissenschaftliche Abteilung*, 30, 1-207.
- Schwerd, K., 1996. Ultraschelvetikum. In: Freudenberger, W. and Schwerd, K.: *Erläuterungen zur Geologischen Karte von Bayern 1:500 000*, pp. 205-210.
- Schwerd, K. and Risch, H., 1983. Zur Stratigraphie und Herkunft der Feuerstätter Decke im Oberallgäu. *Jahresberichte Mitteilungen der oberrheinischen geologischen Vereinigung Neue Folge* 65, 279-290.

- Shultz, M.R. and Hubbard, S.M., 2005. Sedimentology, stratigraphic architecture, and ichnology of gravity-flow deposits partially ponded in a growth-fault-controlled slope minibasin, Tres Pasos Formation (Cretaceous). *Journal of Sedimentary Research* 75, 440-453.
- Sinclair, H.D. and Tomasso, M., 2002. Depositional evolution of confined turbidite basins. *Journal of Sedimentary Research* 72, 451-456.
- Sissingh, W., 1977. Biostratigraphy of Cretaceous calcareous nannoplankton. *Geologie en Mijnbouw*, 56, 37-65.
- Smith, R., 2004. Silled sub-basins to connected tortuous corridors: sediment distribution systems on topographically complex sub-aqueous slopes. In: Lomas, S.A. and Joseph, P. (Eds.): *Confined Turbidite Systems*. Geological Society London Special Publication 222, pp.23-43.
- Stover, L.E., Brinkhuis, H., Damassa, S.P., de Verteuil, L., Helby, R.J., Monteil, E., Artridge, A.D., Powell, A.J., Riding, J.B., Smelror, M., and Williams, G.L., 1996. Mesozoic-Tertiary dinoflagellates, acritarchs and prasinophytes. In: Jansonius, J., and McGregor, D.C. (Eds.), *Palynology: principles and applications*. American Association of Stratigraphic Palynologists Foundation, Dallas 2, pp.641-750.
- Uchman, A., 1999. Ichnology of the Rhenodanubian Flysch (Lower Cretaceous-Eocene) in Austria and Germany. *Beringeria* 25, 67-173.
- Wagreich, M., Neuhuber, S., Egger, H., Wendler, I., Scott, R., Malata, E. and Sanders, D., 2009. Cretaceous oceanic red beds (CORBS) in the Austrian Eastern Alps: Passive-margin vs. active-margin depositional settings. *Society for Sedimentary Geology Special Publication* 91, pp.69-84.
- Weidich, K.F. and Schwerd, K., 1987. Über den Feuerstätter Flysch im Allgäu. *Neues Jahrbuch für Geologie und Paläontologie Abhandlungen* 174, 193-212.
- Wessely, G., 1987. Mesozoic and Tertiary evolution of the Alpine-Carpathian foreland in eastern Austria. *Tectonophysics* 137, 45-59.
- Widder, R.W., 1988. Zur Stratigraphie, Fazies und Tektonik der Grestener Klippenzone zwischen Maria Neustift und Pechgraben/O.Ö. *Mitteilungen Gesellschaft der Geologie- und Bergbaustudenten Österreichs* 34/35, 79-133.
- Zachos, J.C., Röhl, U., Schellenberg, S.A., Sluijs, A., Hodell, D.A., Kelly, D.C., Thomas, E., Nicolo, M., Raffi, I., Lourens, L. J., McCarren, H. and Kroon, D., 2005. Rapid acidification of the ocean during the Paleocene-Eocene thermal maximum. *Science* 308, 1611-1615.
- Ziegler, P.A., 1987. Late Cretaceous and Cenozoic intra-plate compressional deformations in the Alpine foreland – a geodynamic model. *Tectonophysics* 137, 389-420.
- Ziegler, P.A., Bertotti, G., and Cloething, S., 2002. Dynamic processes controlling foreland development - the role of mechanical (de)coupling of orogenic wedges and forelands. In: Bertotti, G. et al. (eds.): *Continental collision and the tectonosedimentary evolution of forelands*. EGU Stephan Müller Special Publication Series 1, pp.17-56.

Received: 6. January 2010

Accepted: 12. May 2009

Hans EGGER¹⁾ & Omar MOHAMED²⁾³⁾

¹⁾ Geological Survey of Austria, Neulinggasse 38, 1030 Vienna, Austria;

²⁾ University of Graz, Institut of Earth Sciences, Heinrichstraße 26, 8010 Graz, Austria;

³⁾ Geology Department, Faculty of Science, El-Minia University, El-Minia, Egypt;

⁷⁾ Corresponding author, hans.egger@geologie.ac.at